ELSEVIER

Thermochimica Acta 297 (1997) 101–107

thermochimica acta

Polymers from renewable resources: XXII: Studies on synthesis and thermal properties of interpenetrating polymer networks derived from castor oil–isophorone diisocyanate–cardanyl methacrylate/poly (cardanyl methacrylate)

D. Das, S.S. Nayak, S.K. Das, P.L. Nayak, S. Lenka*

Department of Chemistry, Ravenshaw College, Cuttack-753003 Orissa, India

Received 30 July 1996; accepted 5 February 1997

Abstract

A large number of interpenetrating polymer networks (IPNs) based on polyurethane of castor oil and isophorone diisocyanate with cardanyl methacrylate and its homopolymer were synthesized using benzoyl peroxide (BPO) as initiator and ethyleneglycol-dimethacrylate (EGDM) as cross-linking agent. The solvent absorptivity behaviour of different IPNs have been studied. The thermal properties have been studied and the kinetic parameters involved in the thermal degradation of the IPNs have been evaluated by using the computerised LOTUS package method. © 1997 Elsevier Science B.V.

Keywords: Polymer; Synthesis; Thermal; Interpenetrating polymer networks

1. Introduction

Initiated by Sperling et al. [1–5], the research work with the interpenetrating polymer network using renewable resources has gained momentum in the current years. Over the years, a large number of papers have been published in this field, relating to the work with the biomonomers derived from the renewable resources. The renewable resources include some of the naturally occurring triglyceride oils such as castor, vernonia and *Lasquerella palmeri*, etc. Orissa is one of the states in India whose forests are crowned with a large number of oil-bearing plants such as castor, tung, vernonia, linseed, crambe, lunaria, cashewnut, etc. The oils of some of the plants contain triglycerides of recenoleic acid. Our laboratory at Ravenshaw College, Orissa, has taken up a programme for the synthesis and characterisation of some high-temperature resistant IPNs from the low-cost oils of Orissa. So, for this purpose cashewnut shell liquid (CNSL) and castor oil have been selectively chosen. The major components of CNSL, i.e. cardanol, cardol, 6-methyl cardol and anacardic acid have been characterised by Tymen [6], Verma et al. [7], using UV, IR, H′-NMR, etc. Cardanyl methacrylate, a derivative of cardanol and its homopolymer have been synthesized following the procedure of Kaliyappan and Kannan [8]. Nayak and Lenka have reported the synthesis and characterisation of some IPNs derived from castor-oil based polyurethane and cardanol-furfural resin [9]. This present communication reports the synthesis of IPNs derived from castor-oil based polyurethane and a new vinyl monomer, i.e. cardanyl methacrylate and its

*Corresponding author. Tel.: 00 91 613523; fax: 0091 0671 614646.

PII S0040-6031(97)00150-0

homopolymer. Thermal analysis has been carried out by using a novel computerised LOTUS package method developed by Rao and Mohanty [10]. This computer analysis with spreadsheet graphic capabilities is found to be the most suitable one for the study of kinetic parameters involved in thermal degradation.

2. Experimental

2.1. Materials

The characteristic values of the castor oil used, such as hydroxyl number, acid number and isocyanate equivalent were determined by the standard procedure. Cardanyl methacrylate was prepared by using earlier methods [8]. All the chemicals used in this investigation were of analytical grade. The vinyl monomer was made free from inhibitor before use. The benzoyl peroxide was recrystallised from chloroform.

2.2. Synthesis of polyurethane (PU)

Castor oil (1 mol) was added to isophorone diisocyanate (1.6 mol) to maintain the NCO/OH ratio at 1.6. The above reaction was carried out at 45°C with continuous stirring for 1 h till the viscous prepolymer (polyurethane) separated out. The other PU with the molar ratio of 1.8 was also prepared following the same procedure.

2.3. Synthesis of interpenetrating polymer network (IPN)

The mixtures of PU and cardanyl methacrylate/poly (cardanyl methacrylate) with different weight-to-weight ratios (25 : 75, 35 : 65) in methylethylketone (MEK) were taken in a round bottom flask. Then, 5 ml of 10% EGDM along with 20 mg of BPO were added to each mixture and stirred for 15 min to form a homogeneous solution. Following that, the temperature was raised to 75°C to initiate polymerisation with continuous stirring for 1 h till the formation of a thick solution. The solution was poured into a glass mould and kept in a preheated oven at 75°C for 24 h. The films thus formed were cooled slowly and removed from the mould. The feed composition data of the IPNs is furnished in Table 1.

Table 1
Feed composition data of IPNs

Sample code	System	NCO/OH	PU/CM or PCM [d]
IPN-1	CO[a] + IPDI[b] + CM[c]	1.6	25 : 75
IPN-2	CO + IPDI + CM	1.6	35 : 65
IPN-3	CO + IPDI + CM	1.8	25 : 75
IPN-4	CO + IPDI + CM	1.8	35 : 65
IPN-5	CO + IPDI + PCM[d]	1.8	35 : 65

[a]Castor oil.
[b]Isophorone diisocyanate.
[c]Cardanyl methacrylate.
[d]Poly (cardanyl methacrylate).

2.4. Solvent absorptivity behaviour of IPNs

Each of the IPNs was stored in 3 cm^3 of different solvents for 16 h. Excess of the solvent present on the surface of the IPN was removed with a filter paper. Then, it was weighed and the absorptivity of solvent (SA%) was calculated using the following equation:

$$SA\% = \frac{W_2 - W_1}{W_1} \times 100$$

where W_1, is the weight of the dry sample and W_2 the weight of the sample after absorption of the solvent. The data are furnished in Table 2.

2.5. Methods of measurement

Infrared spectra were measured on a Perkin–Elmer IR spectrometer. Thermal analysis was carried out using a Ray Saxton; Perkin–Elmer 7-series thermal analyser at a heating rate of 10 K min^{-1} in nitrogen atmosphere.

Table 2
Solvent absorptivity of IPNs

	SA% for different IPNs				
Solvent	IPN-I	IPN-2	IPN-3	IPN-4	IPN-5
Distilled water	2.4	1.8	2.1	1.6	3.6
Chloroform	3.2	2.6	2.8	2.0	4.8
Toluene	40.4	36.5	39.I	28.6	60.2
Methylethylketone	60.6	54.2	50.4	40.8	76.0

3. Results and discussion

The IPNs were synthesized by reacting the polyurethane of castor oil and IPDI with cardanyl methacrylate/ poly (cardanyl methacrylate) in the presence of BPO as initiator and EGDM as cross-linker. The macromolecular structure of the IPNs are highly cross-linked. An expected reaction scheme and the structure of IPNs may be interpreted as given in Scheme 1.

3.1. FTIR spectra

The IR spectrum of cardanyl methacrylate given in Fig. 1(a) shows the characteristic carbonyl stretching frequency of ester group at ca. 1750 cm^{-1}. This is at a higher frequency than the normal ester C=O stretch due to phenyl conjugation with alcohol oxygen. Two strong bands at 1320 and 1290 cm^{-1} are due to C–O

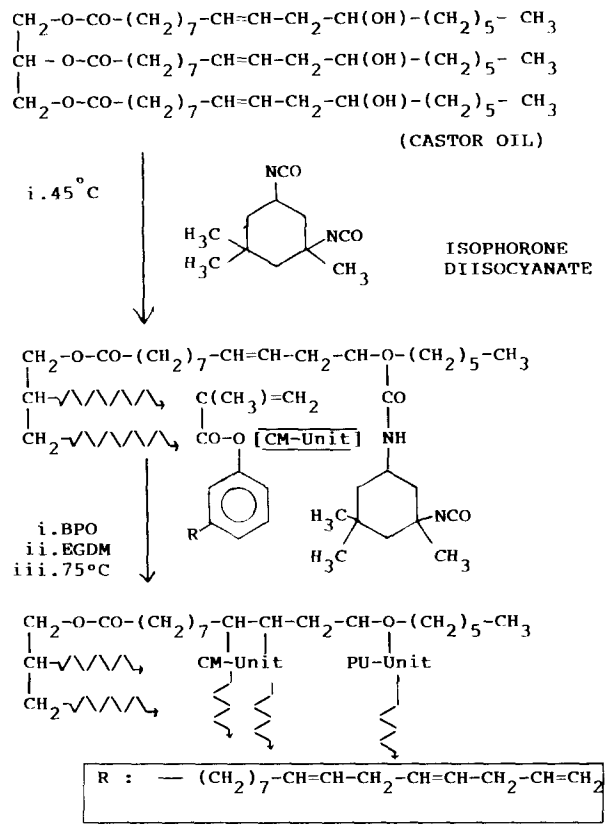

Scheme 1. Synthesis and an expected crosslinked structure of IPN.

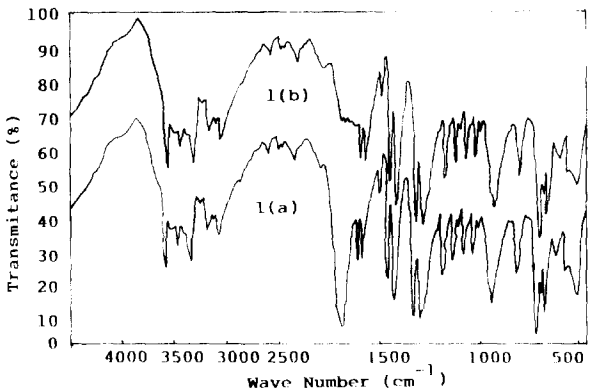

Fig. 1. (a) – IR spectra of cardanyl methacrylate; and (b) – IR spectra of poly (cardnyl methacrylate).

stretching. The presence of a peak of moderate intensity at 1640 cm^{-1} indicates C=C stretching mode of methacrylate moiety. Two bands at 2962 and 2872 cm^{-1} indicate C–H stretching of the methyl group. The C–H stretching vibration of the unsaturated part of the side chain was observed at 3020 cm^{-1}. In the polymer Fig. 1(b), the peak at 1650 cm^{-1} was not observed due to the conversion of methacrylate C=C to C–C, whereas the peak at 3020 cm^{-1} did not change. It indicates that the side chain of monomer with its double bond remains intact in the polymer, and polymerisation takes place only at the methacrylate double bonds.

3.2. Thermal analysis

Thermogravimetry is a technique in which mass of the specimen under investigation is continuously followed as a function of temperature and time as it is heated or cooled at the predetermined rate. Sbirrazzouli et al. [11] have discussed the validity and application of different methods. Satava [12] developed a graphical method for comparison of log $g(\alpha)$ with log $p(x)$. This method is based on the principle of the rate of decomposition expressed as $d\alpha/dt = kf(\alpha)$, where α = rate of heating, 'K' the rate constant and $f(\alpha)$ depends upon the mechanism. All these procedures have a number of sequential calculations which have proved to be cumbersome and, hence, resulted in the use of computers in this field. Several packages [13,14] have been developed, mainly using either FORTRAN or BASIC compilers

for the determination of the kinetic mechanism of decomposition. Recently, Rao and Mohanty [10] have developed a new computer analysis method, involving spread sheets with built-in graphic capabilities for thermogravimetric analysis. To illustrate the capabilities of spread sheets, LOTUS 123 was chosen for analysis of data. Necessary cell functions for different temperatures, using regression analysis as suggested by Nair and Sundarar [15], is carried out for $1/T$ and log $g(\alpha)$. The regression value is given by

$$R^2 = \frac{(XY - n\bar{X}\bar{Y})^2}{(X^2 - n\bar{X}^2)(Y^2 - n\bar{Y}^2)}$$

The slope is given by

$$b = XY - n\bar{X}\bar{Y}/Y^2 - n\bar{Y}^2$$

The constant is given by, $a = \bar{Y} - b\bar{X}$, where $X = 1/T$, $Y = \log\ g(\alpha)$ and 'n' the number of observations. The fourteen kinetic mechanisms considered are given in Table 3. The mechanism which has R^2 value close to unity is choosen. The programme evaluates the values for log $g(\alpha)$. It gives the results of slopes, constants, R^2 values corresponding to each of the mechanism and prints out the result. We have used the Coats and Redfern and the Riech method for the determination of kinetic parameters. The equations for the two foregoing methods are represented as follows.

3.3. The Coats and Redfern method

$$\ln[G(\alpha)/T^2] = \ln\frac{AR}{\beta E}\left(1 - \frac{2RT}{E}\right) - \frac{E}{2.3R} \times 1/T$$

where α = rate of heating, R = gas constant, $A = Z$ = collision frequency factor, E = activation energy. 'E' is calculated from the straight line obtained by plotting $\ln[\alpha/T^2]$ vs. $1/T$ and $\ln A$ can be obtained from the intercept.

3.4. The Riech method

$$\ln[G(\alpha)] = -\frac{E}{R} \times \frac{1}{T} + \ln\left[\frac{R}{E} \times \frac{A}{\beta} \times T_n^2\right]$$

where 'n' is the number of observations. The thermograms of five typical IPNs are presented in Figs. 2 and 3.

The data showing the percentage decomposition of the various IPNs at different temperatures is furnished in Table 4.

From the thermograms given in Figs. 2 and 3 the thermal degradation of the IPNs are studied in

Table 3
Kinetic function (integro-differential forms) used for the data analysis

Function	Name of the function	$g(\alpha)$	$f(\alpha)$	Rate controlling process
MPL^1	Mampel power law, $n = 1$	$-\ln(1-\alpha)$	$(1-\alpha)$	Chemical reaction
MPL^0	Mampel power law, $n = 0$	α	1	Chemical reaction
$MPL^{1/3}$	Mampel power law, $n = 1/3$	$3[1-(1-\alpha)^{1/3}]$	$(1-\alpha)^{1/3}$	Chemical reaction
$MPL^{1/2}$	Mampel power law, $n = 1/2$	$2[1-(1-\alpha)^{1/2}]$	$(1-\alpha)^{1/2}$	Chemical reaction
$MPL^{2/3}$	Mampel power law,$n = 2/3$	$3/2[1-(1-\alpha)^{2/3}]$	$(1-\alpha)^{2/3}$	Chemical reaction
MPL^2	Mampel power law, $n = 2$	$(1-\alpha)^{-1} - 1$	$(1-\alpha)^2$	Chemical reaction
R_2	Contracting cylinder	$1-(1-\alpha)^{1/2}$	$2(1-\alpha)^{1/2}$	Phase-boundary reaction, symmetry
R_3	Contracting sphere	$1-(1-\alpha)^{1/3}$	$3(1-\alpha)^{2/3}$	Phase-boundary reaction, spherical symmetry.
A_2	Avrami–Erofeev equation $n = 2$	$(n=2)[-\ln(1-\alpha)]^{1/2}$	$2(1-\alpha)[-\ln(1-\alpha)]^{1/2}$	Assumes random nucleation and its subsequent growth, $n = 2$
A_3	Avrami–Erofeev equation $(n = 3)$	$[-\ln(1-\alpha)]^{1/3}$	$3(1-\alpha)[-\ln(1-\alpha)]^{2/3}$	Assumes random nucleation and its subsequent growth, $n = 3$.
A_4	Avrami–Erofeev equation $(n = 4)$	$[-\ln(1-\alpha)]^{1/4}$	$4(1-\alpha)[-\ln(1-\alpha)]^{3/4}$	Assumes random nucleation and its subsequent growth, $n = 4$
D_2	Valensi (Barrer) Equation	$\alpha + (1-\alpha)\ln(1-\alpha)$	$[1-\ln(1-\alpha)]^{-1}$	Two-dimensional difusion, cylindrical symmetry,
D_3	Jander Equation.	$[1-(1-\alpha)^{1/3}]^2$	$3/2(1-\alpha)^{2/3}$	Three-dimensional diffusion.
D_4	Ginstling–Boknshtein equation.	$1-2\alpha/3-(1-\alpha)^{2/3}$	$3/2[(1-\alpha)^{-1/3}-1]^{-1}$	Three-dimensional diffusion, spherical symmetry.

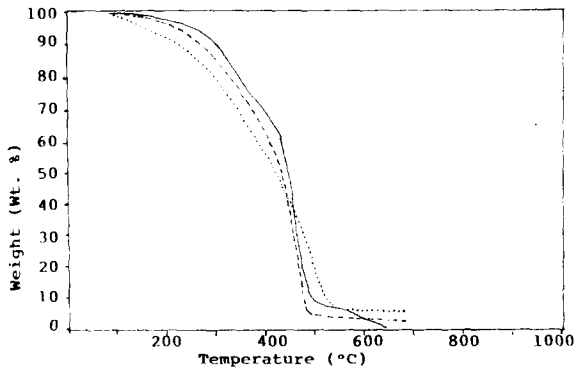

Fig. 2. TG curve of IPN-1, IPN-2 and IPN-3: (———) – IPN-1; (- - -) – IPN-2; and (· · ·) – IPN-3).

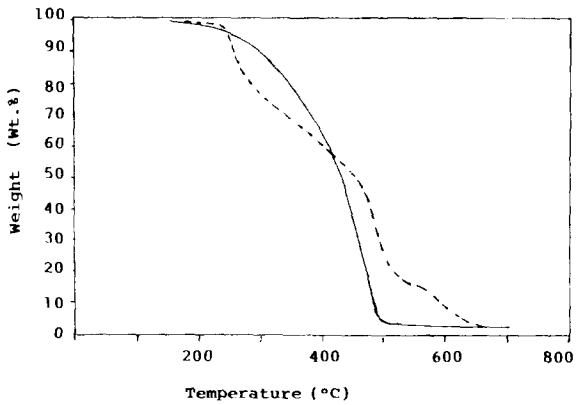

Fig. 3. TG curve of IPN-4 and IPN-5: (———) – IPN-4; and (- - -) – IPN-5.

different temperature ranges. The thermal degradation of the first four IPNs are studied in three distinct ranges, i.e. (150–250), (250–400) and (400–500)°C, whereas for the fifth IPN another range, namely (500–600)°C is chosen.

3.5. *The first stage of thermal degradation (150–250°C)*

The first four IPNs show a weight loss of ca. 10% in this range. This is due to the removal of moisture contained in the sample. IPN-3 and IPN-4 show the weight loss after 250°C, whereas the same for IPN-1 and IPN-2 occur at a relatively lower temperature, i.e. 200°C. This may be attributed to the fact that due to higher molar ratio of diisocyanate (1.8) in IPN-3 and IPN-4, the system becomes more rigid. So the water molecules present in the macromolecular volume during synthesis do not get easily free. But IPN-5, which is synthesised after homopolymerisation of vinyl monomer, is less cross-linked and shows a weight loss of ca. 25% in this range. The swelling measurement as furnished in Table 2 also lies in good agreement with the above fact when the IPN-3 and IPN-4 are less solved and the IPN-5 is most solvated.

3.6. *The second stage of thermal degradation (250–400°C)*

In this temperature range, the unreacted unsaturated parts (=bonds) get activated due to the presence of the excess of BPO in the macromolecule. So recross-linking occurs in case of IPNs which make the system more rigid. The new cross-links formed inside the macromolecules develop a strain in the molecular chains. So the small groups present outside the macromolecular structure are released which leads to a weight loss of ca. 40%.

3.7. *The third stage of thermal degradation (400–500°C)*

In this temperature range, the strained macromolecule (IPN-1 to IPN-4) suffers depolymerisation, lead-

Table 4
Thermal data of IPNs

Sample code	System	Decomposition % at various temperature ranges				
		100–200	200–300	300–400	400–500	500–600
IPN-1	CO + IPDI + CM	2	8.5	30	90	95
IPN-2	CO + IPDI + CM	1.5	11	32	94	94
IPN-3	CO + IPDI + CM	0	6	38	94	95
IPN-4	CO + IPDI + CM	0	11.5	35	95	95
IPN-5	CO + IPDI + PCM	2	26	44	80	95

ing to the segmental release of larger groups. Hence, a weight loss of ca. 90% occurs in this range. The rigid prepolymeric part (PU) is left as the char residue. The IPN-5 which is less interlinked gets further cross-linked in this range with a simultaneous unzipping of the cross-linked parts which shows a relatively lower weight loss of ca. 80%.

3.8. *The fourth stage of thermal degradation (500–600°C)*

This step is only considered for IPN-5, where the depolymerisation continues up to the point where 5% of the char residue is left. This attributes the higher thermal stability of IPN-5 as compared to the other IPNs.

3.9. *Interpretation of kinetic parameters*

The Tables 5 and 6 give the Coats and Redfern, and the Riech treatment of kinetic parameter for the degradation of the IPNs. A perusal of the results in Tables 5 and 6 indicates that the IPNs decompose in three distinct steps (Except IPN-5). The activation energy for the second step is higher, which suggests that the recross-linking occurs at a slowest rate. The activation energy for the third step is lower which suggests that the depolymerisation occurs at a faster rate. This is in good agreement with the thermogram patterns (Figs. 2 and 3) which show a sharp weight loss in the (400–500)°C range. For IPN-5, the sharp weight loss occurs after the third stage. This is evident from the lower activation energy of the last stage with respect to third step.

Table 5
Coats and Redfern treatment of kinetic parameters for the thermal degradation of IPNs

Sample	Temperature range	Function	R^2	E (K Cal/mol)
IPN-1	150–250	MPL^2	0.826231	10.46
	250–400	MPL^1	0.995102	15.22
	400–500	D_4	0.984548	8.03
IPN-2	150–250	MPL^2	0.854980	15.77
	250–400	D	0.992646	18.87
	400–500	MPL^0	0.969101	10.045
IPN-3	150–250	D_4	0.989646	27.77
	250–400	D_4	0.499139	23.98
	400–500	MPL^0	0.995690	8.762
IPN-4	150–250	D_2	0.995294	28.43
	250–400	D_3	0.997960	27.56
	400–500	D_4	0.986708	25.92
IPN-5	150–250	MPL^0	0.854407	8.59
	250–400	D_2	0.960113	6.318
	400–500	A_2	0.991592	18.11
	500–600	D_4	0.9777576	10.23

Table 6
L. Riech treatment of kinetic parameters for the thermal degradation of IPNs

Sample	Temperature range	Function	R^2	E (K Cal/mol)
IPN-1	150–250	MPL^2	0.858680	17.14
	250–400	R_3	0.995605	20.61
	400–500	R_2	0.9869554	10.50
IPN-3	150–250	D_2	0.995877	30.44
	250–400	D_3	0.998353	30.01
	400–500	$MPL^{1/3}$	0.989458	13.15
IPN-5	150–250	MPL^0	0.874815	47.67
	250–400	MPL^0	0.990430	3.19
	400–500	A_3	0.995114	18.84
	500–600	MPL^0	0.989015	12.8

Acknowledgements

The authors thank the University Grant Commission, New Delhi, for offering a fellowship to one of the authors (D. Das). Thanks are due to Dr. M.K. Mishra, Texaco R and D, USA, for the characterisation of samples (TGA/IR).

References

[1] L.H. Sperling, C.E. Carraher, S.P. Qureshi, J.A. Manson and L.W. Barrett, in C.G. Gebellin (Ed.), Polymers from Biotechnology, Plenum Press, New York, 1991.
[2] L.H. Sperling, J.A. Manson and M.A. Linne, J. Polym. Material, I (1984) 54.
[3] L.H. Sperling and J.A. Manson, J. Am. Oil Chem. Soc., 60 (1983) 1887.
[4] L.W. Barrett and L.H. Sperling, Polymer Engg. and Science, 33(14) (1993) 913.
[5] L.W. Barrett and L.H. Sperling, PMSE Preprints, J. Polym. Sci., 65 (1991) 345.
[6] J.H.P. Tyman, Chem. Soc. Rev., 8 (1979) 499.
[7] I.K. Verma, S.K. Dhara, M. Verma and T.S. Biddapa, Angew, Makromol. Chem., 154 (1987) 67.

[8] T. Kaliyappan and P. Kannan, J. Polym. Matter, 11 (1994) 121–128.
[9] D.K. Mishra, D. Parida, S.S. Nayak, S. Lenka and P.L. Nayak, Macromol. Reports, A32(Suppl. 4) (1995) 499–510.
[10] K.K. Rao and S. Mohanty, Proc. 8th National Workshop on Thermal Analysis, India, 1991, p. 236.
[11] N. Sbirrazzauoli, D. Brunel and L.E. Legant, J. Therm. Anal., 38 (1992) 1509.
[12] V. Satava and F. Skavara, Mechanisms and kinetics of decomposition of solids by thermogravimetric method, J. Am. Chem. Soc., 52 (1969) 591–595.
[13] C.D. Doyle, J. Appl. Polym. Sci., 6 (1962) 639.
[14] S. Ma and K.N.I.S., A Computer Programme for the systematic kinetic analysis of non-isothermal thermogravimetric data, Thermochim. Acta, 184 (1991) 233–241.
[15] C.G.R. Nair and C.M. Madhusundaran, Thermal decomposition of the mechanism of decomposition of some transition metal complexes, Thermochim. Acta, 14 (1976) 373.